

Preliminary results of a physical phantom for quantitative assessment of breast MRI

M. Freed^{1,2}, J. A. de Zwart³, J. T. Loud⁴, R. H. El Khoulfi⁵, M. H. Greene⁴, B. D. Gallas¹, K. J. Myers¹, J. H. Duyn³, D. A. Bluemke⁵, and A. Badano¹
¹CDRH/OSEL/DIAM, FDA, Silver Spring, MD, United States, ²Department of Bioengineering, University of Maryland, College Park, Maryland, United States, ³NINDS/LFMI/Advanced MRI Section, National Institutes of Health, Bethesda, MD, United States, ⁴NCI/Clinical Genetics Branch, National Institutes of Health, Rockville, MD, United States, ⁵Department of Radiology and Imaging Sciences, National Institutes of Health, Bethesda, MD, United States

Introduction: Initial reports have demonstrated that dynamic contrast-enhanced (DCE)-MRI may be superior to the current breast cancer screening technique, x-ray mammography, for evaluating the extent of disease and screening patients with high risk or dense breast tissue [1, 2]. However, the technique suffers from suboptimal and highly-variable specificity, which can lead to unnecessary biopsies and increased patient anxiety. In response, there has been a recent effort in the breast MR imaging community towards standardization. A breast MR lexicon has been developed [3], along with a set of standardized quantities and symbols for kinetic analysis of Gd-DTPA tracer washout [4]. Despite this, there remains a lack of standardization of specific MRI protocols for data acquisition. Review papers have discussed the various protocols used and given recommendations regarding which protocol to use for a given clinical scenario [5, 6]. Nevertheless, quantitative assessment of MR protocols and their efficacy for different clinical situations has not yet been adequately addressed. To this end, we are developing a physical, tissue-mimicking phantom to be used for task-based, quantitative assessment of breast MRI protocols. Important requirements for such a phantom include T_1 and T_2 relaxation parameters similar to those in human tissue and a random background structure that mimics anatomical variations in patient populations. Here we present initial results of the physical phantom characterization and comparison to human data.

Methods: Phantom construction. The phantom was constructed using lard to simulate adipose tissue and coagulated, fresh egg whites to simulate fibroglandular tissue. The lard was melted on a stirring hotplate until it reached a temperature of 100-110°C. Then egg whites, mixed with a preservative, were added and allowed to mix with the lard at a constant stirring speed for about 30 seconds. The mixture was then cooled at room temperature in a sealed plastic jar. This procedure resulted in a random structure with separate adipose- and fibroglandular-mimicking compartments.

T_1 and T_2 estimation. T_1 and T_2 relaxation times of the lard and egg compartments of the phantom were estimated using maximum-likelihood estimation with Rician noise probability distribution functions [7]. Scans were performed on a Siemens Magnetom 1.5T clinical scanner using a knee coil. For lard, T_1 and T_2 values were estimated on a tube of solid lard assuming monoexponential signal behavior. The T_1 and T_2 values of the egg compartment were estimated on the actual phantom using a double exponential signal equation. In this equation, the lard T_1 and T_2 as estimated above were fixed, and the egg/lard mixing fraction was an additional free parameter for each voxel. Both the lard tube and actual phantom were imaged simultaneously using an inversion recovery sequence for T_1 ($TI=[22,35,45,75,100,150,200,250,400,500,600,900,1000,1500,2500,4500]$ ms, $res=2.5 \times 2.5 \times 2.5$ mm³, $TR=25$ s) and a spin-echo sequence with similar parameters for T_2 estimation

($TE=[15,20,25,30,35,40,50,70,75,95,100,120,150,200,300]$ ms).

Background structure. Anonymous, archived patient data ($n=71$) from a 1.5T Phillips scanner acquired with a dedicated breast coil using a fat-suppressed, T_1 -weighted, pre-contrast scan were analyzed (in-plane resolution = 0.586-0.664 mm, slice thickness = 1.9-2.3 mm) and compared with phantom data ($n=20$) acquired with the same sequence, coil, and scanner type. Background structure was statistically quantified using 2D covariance kernels [8], which are a measure of the size and shape distribution of objects in the images. The covariance kernel was normalized by the pixel variance to account for system variations.

Results: Fig. 1 shows the custom jar developed for the phantom, as well as T_1 -weighted example images of both the phantom and human data. Qualitatively, the phantom and human images appear similar. Fig. 2 shows a comparison of T_1 and T_2 estimates of the phantom components with published human tissue values [9-11]. Phantom relaxation values fall within 2 times standard error of the human data. Fig. 3 shows the radially-averaged covariance kernel for all of the phantom and patient data with standard error bars. The phantom covariance length is on average slightly longer than that of the patients, but matches the patient covariance within two standard error bars.

Conclusion: We have constructed preliminary physical phantoms for quantitative, task-based evaluation of breast MRI imaging sequences. T_1 and T_2 values of both adipose- and fibroglandular-mimicking compartments match human data. Phantom background structure, as measured by radially averaged covariance kernels, is similar to that of humans. Following further characterization (e.g., water-fat shift validation, extended covariance analysis, additional materials), a kinetic compartment will be added to the phantom to simulate Gd-DTPA tracer wash-out curves.

Acknowledgments: Eugene O'Bryan, Randy Bidinger, Bruce Fleharty for advice on design and manufacturing of the custom jar. Frank Samuelson and Jonathan Boswell for help using the computing cluster. Funding from FDA/OWH. Supported in part by an appointment to CDRH/ORISE.

References: [1] Kuhl. Radiology, 244, 672, 2007. [2] Solin et al. J. Clin. Oncol., 26, 386, 2008. [3] Ikeda et al. J. Mag. Res. Imaging, 13, 889, 2001. [4] Tofts et al. JMRI, 10, 223, 1999. [5] Kuhl. Radiology, 244, 356, 2007. [6] Orel and Schnall. Radiology, 220, 13, 2001. [7] Karlsen, Verhagen, and Bovée. MRM, 41, 614, 1999. [8] Barrett and Myers. Foundations of Image Science, 2004. [9] Merchant et al. Acta Radiologica, 34, 356, 1993. [10] Bottomley et al. Med. Phys., 14, 1, 1987. [11] Rakow-Penner et al. JMRI, 23, 87, 2006.

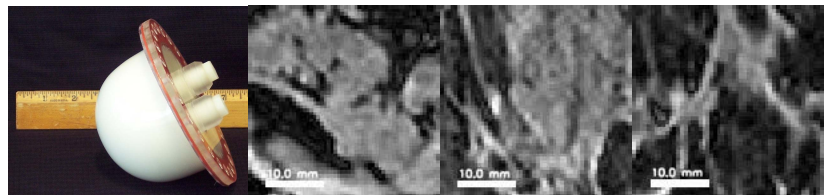


Figure 1. (from left to right) custom jar for phantom production, fat-suppressed, T_1 -weighted images of a phantom, patient, and another patient

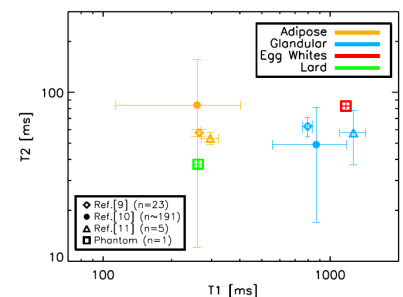


Figure 2. Comparison of phantom T_1 and T_2 values with human data.

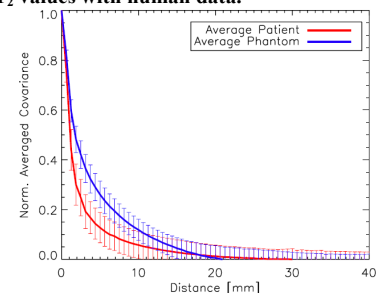


Figure 3. Radial average of the covariance kernel for all human and phantom data.